The Journal of Agricultural Science

cambridge.org/ags

How sequential reduction of terminal electron acceptors modulates nitrification and dynamics of nitrifying bacteria and archaea in a tropical vertisol

Santosh Ranjan Mohanty, Rakhi Yadav, Garima Dubey, Usha Ahirwar, Neha Ahirwar, K. Aparna, D. L. N. Rao and Bharati Kollah

ICAR - Indian Institute of Soil Science, Nabibagh, Bhopal, 462038, India

Crops and Soils Research Paper

Cite this article: Mohanty SR, Yadav R, Dubey G, Ahirwar U, Ahirwar N, Aparna K, Rao DLN, Kollah B (2018). How sequential reduction of terminal electron acceptors modulates nitrification and dynamics of nitrifying bacteria and archaea in a tropical vertisol. *The Journal of Agricultural Science* **156**, 215–224. https://doi.org/10.1017/S0021859618000266

Received: 30 June 2016
Revised: 20 February 2018
Accepted: 16 March 2018

Key words:
Archaea; bacteria; nitrification; TEAPs; vertisol

Author for correspondence:
Santosh Ranjan Mohanty, E-mail: santosh.mohanty@icar.gov.in

Abstract

Nitrification potential of a tropical vertisol saturated with water was estimated during sequential reduction of nitrate (NO_3^-), ferric iron (Fe^{3+}), sulphate (SO_4^{2-}) and carbon dioxide (CO_2) in terminal electron-accepting processes (TEAPs). In general, the TEAPs enhanced potential nitrification rate (PNR) of the soil. Nitrification was highest at Fe^{3+} reduction followed by SO_4^{2-} reduction, NO_3^- reduction and lowest in unreduced control soil. Predicted PNR correlated significantly with the observed PNR. Electron donor Fe^{2+} stimulated PNR, while S^{2-} inhibited it significantly. Terminal-restriction fragment length polymorphism targeting the *amoA* gene of ammonia-oxidizing bacteria (AOB) and ammonia-oxidizing archaea (AOA) highlighted population dynamics during the sequential reduction of terminal electron acceptors. Only the relative abundance of AOA varied significantly during the course of soil reduction. Relative abundance of AOB correlated with NO_3^- and Fe^{2+}. Linear regression models predicted PNR from the values of NO_3^-, Fe^{2+} and relative abundance of AOA. Principal component analysis of PNR during different reducing conditions explained 72.90% variance by PC1 and 19.52% variance by PC2. Results revealed that AOA might have a significant role in nitrification during reducing conditions in the tropical flooded ecosystem of a vertisol.

Introduction

Microbial-mediated nitrification is a key biogeochemical process in the global nitrogen (N) balance. Thus, knowledge of the key players in nitrification and prediction of their activity is essential for environmental and economic reasons. Nitrification of ammonia (NH_3) to nitrate (NO_3^-) is believed to be a two-step process performed by two distinct groups of chemolithoautotrophic microorganisms (Kowalchuk *et al.* 2000). One step oxidizes ammonium (NH_4^+) to nitrogen dioxide (NO_2^-) and another oxidizes NO_2^- to NO_3^-. Most ammonia-oxidizing bacteria (AOB) belong to the *β*-proteobacteria. There are two different clusters of nitrifiers within the *β*-AOB, the *Nitrosomonas* cluster and the *Nitrosospira* cluster. The *Nitrosomonas* cluster includes the genera *Nitrosmonas* and *Nitrosococcus*. Similarly, the nitrosospira cluster includes the genera *Nitrosospira*, *Nitrosolobus* and *Nitrosovibrio*. Nitrite-oxidizing bacteria have been described as four genera; *Nitrobacter*, *Nitrococcus*, *Nitrospina* and *Nitrospira* (Watson *et al.* 1986).

Understanding of the N cycle has been revised in the past few years by the discovery of archaeal nitrification (Jung *et al.* 2011). Archaea is composed of four phyla, *Crenarchaeota*, *Euryarchaeota*, *Korarchaeota* and *Nanoarchaeota*. Ammonia-oxidizing archaea (AOA) are members of a proposed novel phylum *Thaumarchaeota* (Gribaldo *et al.* 2010). However, as they are difficult to cultivate, some aspects of their physiology and contribution to biogeochemical pathways are still speculative. Ammonia-oxidizing archaea are found in almost all environments. Crenarchaeotal 16S rRNA gene sequences have been found from sediments of Pacific and Atlantic oceans (Flood *et al.* 2015), lakes (Yang *et al.* 2016), guts of animals (Radax *et al.* 2012), agricultural soils (Tourna *et al.* 2011) and forest soils (Isobe *et al.* 2012). Typically, AOA greatly outnumber AOB in soils and sediments. In agricultural soils, the archaeal *amoA* gene copy number can be 3000 times higher than the bacterial *amoA* gene copies (Leininger *et al.* 2006).

Nitrification has been studied thoroughly in upland aerobic agricultural soil ecosystems. However, it is unclear how nitrification occurs in soil under flooded conditions. It has been projected that climate change is likely to affect the atmospheric water distribution pattern. Increasing global temperature will intensify precipitation and may lead to the conversion of many uplands to wetlands in tropical countries (Walther *et al.* 2002; Davidson & Janssens 2006). Under this scenario, soil biogeochemical processes will switch from aerobic to anaerobic

CAMBRIDGE UNIVERSITY PRESS

type. In many South Asian countries such as India, agriculture is dependent on monsoon rainfall. During this period, most upland soils remain inundated for several days depending on precipitation intensity, causing the soil to undergo short-term or long-term anaerobiosis. Soils under flooded conditions undergo anaerobiosis with sequential reduction of NO_3^{1-}, Fe^{2+}, SO_4^{2-} and carbon dioxide (CO_2) as the terminal electron-accepting process (TEAP). Reduction and oxidation (redox) of the electron acceptors occurs at different temporal and spatial scales in the oxic and anoxic soil compartments. Exposure of anaerobic soil to oxygen leads to the oxidation of various reduced molecules. Therefore, soil undergoing reduction followed by oxidation can be characterized by different redox species and proportions of anaerobic-aerobic microorganisms. The reduction–oxidation is likely to influence the cycling of most elements. To reveal the complex interaction between redox metabolism and nitrification, experiments were carried out with the following objectives: (1) define nitrification potential of soil (vertisol) during reducing conditions, (2) elucidate the interaction between electron donors and nitrification and (3) evaluate the population dynamics of AOB and AOA during nitrification.

Materials and methods

Soil sampling and characterization

Experiments were carried out using soil samples collected from the experimental fields of the Indian Institute of Soil Science, Bhopal, Madhya Pradesh, India (23.30 N, 77.40 E, 485 m a.s.l.). The soil is a heavy clayey vertisol (*typic* Haplustert) (Mohanty *et al.* 2014), characterized with organic carbon (C) of 5.7 g/kg, available N of 225 mg/kg, available phosphorus (P) of 2.6 mg/kg, available potassium (K) of 230 mg/kg, electrical conductivity (EC) of 0.43 dS/m and pH 7.5. The textural composition of the soil was: sand 15.2%, silt 30.3%, clay 54.5%. The soil had 863.24 μM NO_3^-, 0.01 μM Fe^{2+} and 101.02 μM SO_4^{2-}. After collection, the soils were hand-processed after breaking the clods and removing roots and stones. Soil was then passed through a 2-mm mesh sieve and used within 2 days of collection.

Terminal electron-accepting process and nitrification potential

A total of 18 pre-sterilized serum bottles (capacity 130 ml each) were labelled in triplicate as A, B, C, D, E and F (Fig. 1). The bottles labelled A were used to determine the time points of peak reduction of six terminal electron acceptors. The bottles labelled B, C, D, E and F were used to determine potential nitrification corresponding to five different time points. To each bottle was added 20 g soil and 50 ml sterile double-distilled water to maintain a soil:solution ratio of 1:2.5, and closed with a neoprene septum. Peak period of NO_3^- reduction, Fe^{3+} reduction, SO_4^{2-} reduction and methanogenesis were determined by following the change in concentration of electron acceptors in bottles labelled A. Care was taken to select time points when there was no or minimum overlapping of the TEAPs. The remaining bottles (B–F) were used to measure nitrification potential corresponding to five-time points: time zero (at the beginning of incubation), NO_3^- reduction, Fe^{3+} reduction, SO_4^{2-} reduction and methanogenesis. The experiment was carried out in a completely randomized design. All bottles were kept at 30 ± 2 °C in an incubator with shaking at 100 rotations per minute (rpm) on an orbital shaker. To determine temporal variation of the TEAP, slurry sub-samples were withdrawn from the three bottles at regular intervals and concentrations of NO_3^-, Fe^{3+}, SO_4^{2-} and headspace CH_4 were analysed as described later.

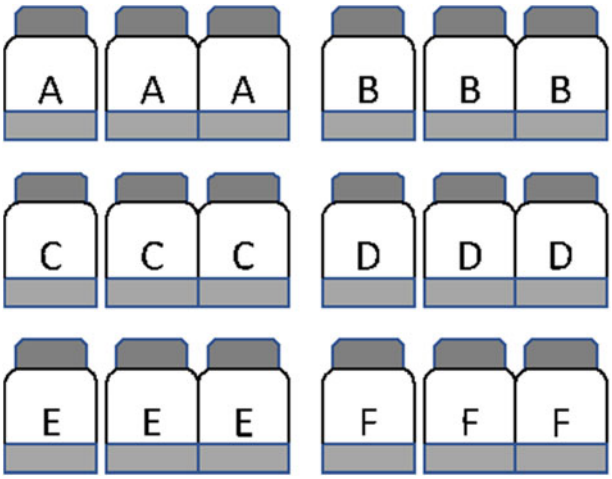

Fig. 1. Microcosms set up to evaluate the effect of redox metabolism on nitrification in the flooded soil ecosystem. Experiments were carried out with three replicates and a total 18 bottles were used. To each bottle, 20 g soil and 50 ml sterile double-distilled water were added. The bottles A were used to determine time points of peak reduction of terminal electron acceptors (NO_3^{1-} reduction, Fe^{3+} reduction, SO_4^{2-} reduction and CH_4 production). At time zero, bottles B were amended with 10 mM NH_4Cl and incubated to determine nitrification by measuring the accumulation of NO_3 over incubation. At the time of peak NO_3^{1-} reduction, bottles C were opened to ambient air and amended with 10 mM NH_4Cl to estimate nitrification. Similarly, bottles D, E, and F were opened at the time of peak reduction of Fe^{3+}, SO_4^{2-}, and CH_4 production and 10 mM NH_4Cl was added to estimate nitrification.

To determine the nitrification potential at the peak reducing phases, three bottles were opened and shaken aerobically at 100 rpm for 2 h to equilibrate headspace with the ambient air. Then NH_4^+ (source: ammonium chloride, NH_4Cl) was added at 10 mM concentration. Bottles were sealed again and incubated at 30 ± 2 °C with shaking at 100 rpm. Slurry sub-samples were withdrawn and NO_3^- concentration was measured daily to determine potential nitrification rate (PNR). The slope of the regression line relating changes in NO_3^- N concentration with incubation time was used to determine the nitrification potential rate (μg NO_3^- produced/g soil/day) (Schmidt & Belser 1982).

Effect of electron donors on nitrification

To understand the effect of electron donors on nitrification, soil samples were incubated with electron donors. These electron donors (Fe^{2+} and S^{2-}) were evaluated because their concentration varied significantly during TEAPs. Briefly, 20-g portions of soil samples were placed in autoclaved 130 ml serum bottles and held under flooded conditions by adding autoclaved distilled water at 1:2.5 volume ratio. Soil slurries were then amended with a freshly prepared aqueous solution of different inorganic electron donors at 10 mM concentration. Soil without any amendment served as a control. The electron donor was either Fe^{2+} (Iron (II) chloride, $FeCl_2$) or S^{2-} (nitrogen sulphide, N_2S). Soil slurries were also amended with NH_4^+ as NH_4Cl (10 mM) to measure nitrification. Bottles were kept in an incubator at 30 ± 2 °C with shaking (100 rpm). Slurry sub-samples were collected periodically and NO_3^- concentration was estimated. Headspace CO_2 concentration was also monitored as described below.

https://doi.org/10.1017/S0021859618000266 Published online by Cambridge University Press

Chemical analysis and potential nitrification rate determination

Concentration of the terminal electron acceptors in the slurry samples was estimated by various wet chemical methods. Soil NO_3^- content was estimated after extraction with calcium sulphate ($CaSO_4$) and reaction by the phenol disulphonic acid method (Jackson 1958). Reduced $Fe^{2+}$was determined by extracting slurries with 0.5 N hydrochloric acid (HCl) and ferrozine assay (Stookey 1970). Sulphate (SO_4^{2-}) content was estimated by extracting slurries with calcium dihydrogen phosphate ($Ca(H_2PO_4)_2$) and turbidometric analysis (Searle 1979).

Quantification of methane and carbon dioxide

Gas samples of 0.1 ml were withdrawn from the headspace of the vials using a gas-tight syringe. After each sampling, the headspace was replaced with an equivalent amount of high purity (>99%) helium (He) to maintain atmospheric pressure. The gas He was used because of its inert chemical nature. Gas analysis was carried out using a gas chromatograph (GC) (CIC, India) equipped with a flame ionization detector and a Porapak Q column (2 m length, internal diameter 3.175 mm, 80/100 mesh, stainless steel column). The injector, column and detector were maintained at 120, 60 and 300 °C, respectively. Gas samples were introduced through the port of an on-column injector. The GC was calibrated before and after each set of measurements using different mixtures of methane (CH_4) in N_2 (Sigma Gases, New Delhi, India) and/or CO_2 in N_2 (Inox Air, Bhopal, India) as primary standards. Methane was quantified with an attached methanizer module. The temperature of the methanizer was 330 °C and the retention times of CH_4 and CO_2 were 1.30 and 2.5 min, respectively.

DNA extraction

DNA was extracted from 0.5 ml of the slurry sample using the ultraclean DNA extraction kit (MoBio, USA) according to the manufacturer's instructions. The DNA concentrations were determined in a biophotometer (Eppendorf, Germany) by measuring absorbance at 260 nm (A260), assuming that 1 A260 unit corresponds to 50 ng of DNA per µl. DNA extraction was further confirmed by electrophoresis on a 1% agarose gel. The extracted DNA was dissolved in 50 µl TE buffer and stored at −20 °C until further analysis.

Polymerase chain reaction amplification

Polymerase chain reaction (PCR) was performed in a total volume of 50 µl containing 1.0 ng of DNA template, 1× PCR buffer (10× PCR buffer II, ABI, CA, USA), 0.2 mM dNTP (Axygen, USA), 1.5 mM $MgCl_2$, 0.1 µM of each primer and 1 U of DNA polymerase (NEB, USA). Thermal cycling was carried out by an initial denaturizing step at 94 °C for 4 min, 35 cycles of 94 °C for 1 min, 56 °C for 30 s, 72 °C for 45 s; final extension carried out at 72 °C for 5 min. The major cycling programme for each primer set is described elsewhere (Francis *et al.* 2005). Fluorescently labelled gene fragments were generated by PCR using 6-carboxyfluorescein labelled at 5′end of the forward primers. The forward primer amoA-1F (5′-GGG GGT TTC TAC TGG TGG T) and the reverse primer amoA-2R (5′-CCC CTC KGS AAA GCC TTC TTC; K = G or T; S = G or C) were used (Caffrey 1995). The primer set targets AOB. The amplicons correspond to positions 332 to 349 and 802 to 822, respectively, of the open reading frame of the *amoA* gene sequence of *Nitrosomonas europaea* (Horz *et al.* 2000). The amo-111F (5′-TTY TAY ACH GAY TGG GCH TGG ACA TC; H = A or C or T; Y = C or T) and amo-643R (5′-TCC CAC TTW GAC CAR GCG GCC ATC CA; W = A or T; R = A or G) primers were used to amplify the *amoA* gene of AOA (Treusch *et al.* 2005). Polymerase chain reaction products were loaded onto a 1% agarose gel to ensure that fragments of the correct size were amplified; they were purified from the reaction mix using a PCR purification kit (Axygen, USA).

Terminal-restriction fragment length polymorphism analysis

Terminal-restriction fragment length polymorphism (TRFLP) analysis was performed on samples for which PCR product was generated. Fluorescently labelled PCR products (100 ng) were digested separately with three restriction enzymes (TaqI, HhaI, HaeIII) for AOB. Similarly, AOA digestion was performed with Msp, HhaI and RsaIII. The restriction enzymes were selected based on the ISPaR tool of the Microbial Community Analysis (MiCA) online resource (http://mica.ibest.uidaho.edu/trflp.php; Shyu *et al.* 2007). Samples were digested with each restriction enzyme by incubating the purified PCR product at 37 °C for 3 h. After digestion, the enzymes were inactivated by incubating the digested samples at 65 °C for 20 min as per the manufacturer's instruction (New England Biolabs, USA). The digested products were sent for fragment analysis at Macrogen (Korea). Aliquots (2–5 µl) of digest were mixed with 2.0 µl formamide and 0.5 µl of an internal length standard Liz 500 (Applied Biosystems, USA). The samples were denatured at 94 °C for 5 min and immediately placed on ice until loading onto genetic analyser (3500, Applied Biosystems, USA). Electrophoresis data were analysed using the GeneScan software (version 1.0, Applied Biosystems, USA). Fragments between 30 and 600 bp were included in the analysis. The area of each peak was expressed as a percentage of the total peak area. Peaks comprising <1% of the total area were removed from the analysis. Profiles were exported and data normalized to minimize error. The relative abundances of individual terminal-restriction fragments (TRFs) in a given PCR product were calculated based on the peak areas of the individual TRF in relation to the total peak area of all TRFs detected in the respective TRFLP community fingerprint pattern.

Phylogenetic assignment of terminal-restriction fragments

The putative phylogenetic identities of the AOA and AOB were determined by use of several web-based programs. Full-length *amoA* gene sequences were downloaded from the National Center for Biotechnology Information (NCBI, Bethesda, MD, USA). *In silico* PCR and DNA restriction were performed using ISPaR (Shyu *et al.* 2007). The *in silico* digestion generated TRFs representing different AOB and AOA. The primers and restriction enzymes used for *in silico* ISPaR were the same as for the *invitro* PCR and TRFLP analysis. The TRF nomenclature was based on the *in silico* analysis of fragment data using the web-based program APLAUS-MiCA (http://mica.ibest.uidaho.edu/trflp.php). The predicted TRFs were imported into PAT (MiCA) and matched with the TRFs generated from the samples. The normalized relative abundance of each TRFs was calculated by the APLAUS tool of MiCA (Shyu *et al.* 2007).

https://doi.org/10.1017/S0021859618000266 Published online by Cambridge University Press

Statistical analysis

All statistical analyses were carried out using the 'agricolae' (De Mendiburu 2014) and 'vegan' (Oksanen *et al.* 2007) packages of the statistical software R (2.15.1) (Ihaka & Gentleman 1996). Results for the experiments were presented as arithmetic means of triplicate samples. Significant difference among the treatments for a given parameter was tested by an analysis of variance (ANOVA) followed Tukey's HSD at $P < 0.05$. Effect of factors (NO_3^-, Fe^{2+}, SO_4^{2-}, CH_4) on the variables (nitrification, relative fluorescence of TRFs), was tested by ANOVA. A linear regression model was developed to define the relationship between PNR and the variables. The confidence level of the regression model was evaluated with r^2 and $P < 0.05$. Complex interaction between electron acceptors and nitrification was derived by multiple regression models. For the interaction, the independent variable was PNR and dependent variables were NO_3^-, Fe^{2+}, SO_4^{2-} and CH_4. The predicted PNR was correlated with observed PNR to test the significance of variation. After natural log transformation and normalization of data, Principal component analysis (PCA) was carried out to identify the major factor and the complexity of interaction. Principal component analysis was interpreted graphically by constructing a biplot, with the original variables drawn as vectors that summarize the inter-correlation between the variables. Principal component analysis biplots are a convenient way of mapping the original variables because the angles of the biplots depict the direction of correlation and the length depicts the amount of correlation. A biplot was made using the values of three replicated observations.

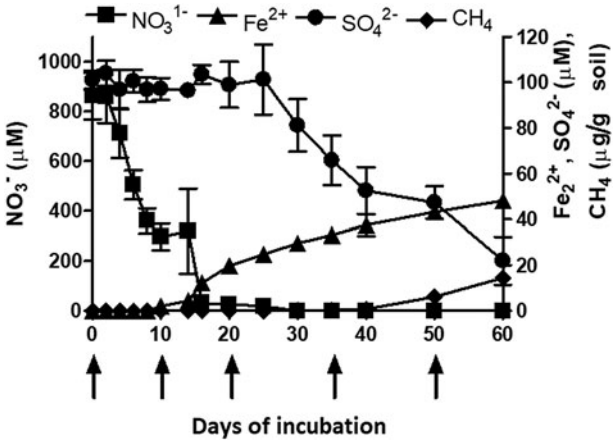

Fig. 2. Microbial redox metabolism or sequential reduction of terminal electron acceptors in a vertisol under flooded moisture regime (Top). Left Y axis represent NO_3^- (square) concentration, while, right *Y*-axis represents Fe^{2+} (triangle), SO_4^{2-} (sphere), and CH_4 (diamond) concentration. X axis represents days of incubation. Each datapoint represents the arithmetic mean and standard deviation of three replicated observations. Arrows indicate time points (0d, 8d, 20d, 35d, 50d) of peak terminal electron-accepting processes when the slurries were incubated further to determine potential nitrification rate.

Results

Terminal electron-accepting processes

The redox metabolism or the TEAPs followed a classical sequential reduction. The reduction metabolism proceeded with NO_3^- reduction, Fe^{3+} reduction, SO_4^{2-} reduction and CO_2 reduction (methanogenesis) (Fig. 2). Nitrate reduction was initiated 2 days after flooding and completed within 2 weeks. A total of 800 µM $NO_3^-$was reduced during denitrification. Iron (Fe^{3+}) reduction was initiated after 10 days. Concentration of Fe^{2+} increased to 45 µM over 60 days. Sulphate reduction was initiated during the 35 days of incubation. Initial SO_4^{2-} concentration was ~95 µM and declined to 25 µM at 60 days of incubation. Methane production was initiated after 40 days of incubation. The cumulative value of CH_4 production was 14.59 µg/g soil after 60 days of incubation. The time points of peak TEAPs were 10, 20, 35 and 50 days representing NO_3^- reduction, Fe^{3+} reduction, SO_4^{2-} reduction and methanogenesis, respectively.

Nitrification during sequential reduction process

Unreduced slurry (0 day) gave 1.33 mM NO_3^-over 30 days of incubation. Contrastingly, NO_3^- reducing and Fe^{3+} reducing slurries resulted in 2.15 and 3.9 mM of NO_3^-, respectively. Potential nitrification rate at different ion reducing phases (at peak TEA concentration) followed the trend of Fe^{3+} reducing >SO_4^{2-} reducing >CO_2 reducing > NO_3^- reducing > unreduced soil (Fig. 3). The PNR of the unreduced slurry was 0.23 µg NO_3^-produced/g soil/day and it increased 14-fold during the Fe^{3+} reduction phase over the unreduced slurry (Table 1).

Effect of electron donors on nitrification

Presence of Fe^{2+} stimulated nitrification, while, S^{2-} inhibited this process (Fig. 4). Nitrification was initiated 15 days after Fe^{2+} addition. A sum of 55 µM $NO_3^-$was produced in the soil amended with Fe^{2+}. Potential nitrification rates of the un-amended control and Fe^{2+} amended soil were 0.196 and 1.63 µg NO_3^- produced/g

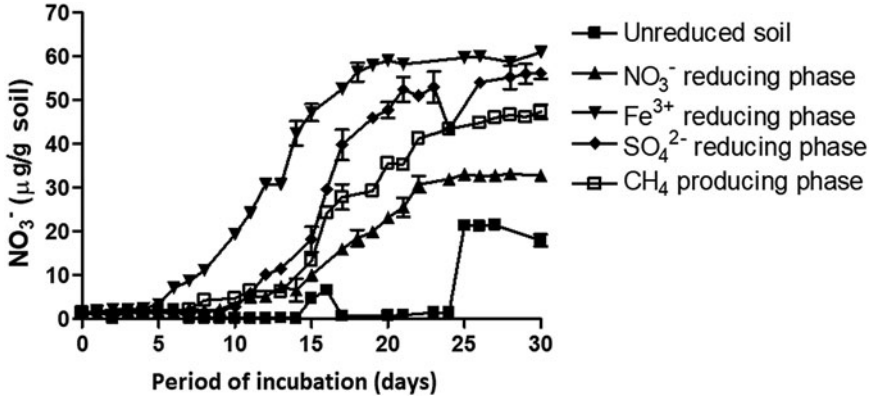

Fig. 3. Nitrification in differently reduced slurry samples. Slurries were incubated for a period of 30 days to determine potential nitrification rate. Each datapoint represents arithmetic mean of three replicated observations with standard deviation as error bar.

https://doi.org/10.1017/S0021859618000266 Published online by Cambridge University Press

Table 1. Potential nitrification rate (PNR) of a vertisol during sequential reduction of terminal electron acceptors. For all samples $n = 3$ and $P < 0.01$

Sequential reduction phase	Peak concentration period (days after incubation) of the terminal electron acceptors	PNR (μg NO_3^- produced/g soil/day)
Unreduced slurry	0	0.23 ± 0.003
NO_3^- reduction	10	1.4 ± 0.10
Fe^{3+} reduction	20	3.12 ± 0.025
SO_4^{2-} reduction	35	2.5 ± 0.13
CH_4 production	50	2.1 ± 0.10

NO_3^-, nitrate; Fe^{3+}, ferric iron; SO_4^{2-}, sulphate; CH_4, methane.

Table 2. Influence of electron donor on the potential nitrification rate (PNR) and cumulative CO_2 production in soil (vertisol)

Redox moieties	Speciation of electron donors	PNR (μg NO_3^- produced/g soil/day)	Cumulative headspace CO_2 (μg/g soil 30/day)
Control	None	0.196 ± 0.042	238 ± 11.9
Electron donor	Fe^{2+}	1.630 ± 0.018	826 ± 43.6
	S^{2-}	0.015 ± 0.001	82 ± 8. 4

Soil samples were incubated with electron donors and PNR was determined from the rate of increase of NO_3^- over incubation period of 30 days. For all samples $n = 3$ and $P < 0.01$. NO_3^-, nitrate; CO_2, carbon dioxide.

soil/day, respectively. Soil amended with S^{2-} exhibited the lowest nitrification activity as it failed to produce any measurable amount of NO_3^-. Potential nitrification rates with Fe^{2+} and S^{2-} were 8.31 times higher and 13 times lower, respectively, than the un-amended control (Table 2). Production of CO_2 was stimulated by addition of Fe^{2+} and was inhibited by S^{2-} ($P < 0.01$) (Table 2).

Terminal-restriction fragment length polymorphism analysis of nitrifying microbial community

The AOB-specific TRFs were of 48 bp, 219 bp and 283 bp (Fig. 5). These TRFs were affiliated to *Nitrosomonas*, *Nitrososcoccus and Nitrosospira*. The AOA-specific TRFs were of 56 bp and 247 bp. These TRFs represented *Crenarchaeota* clade 1.1a and 1.1b (Ying *et al.* 2010). The *in silico* nomenclature was tentative because the TRFs were not confirmed through sequencing of the fragments. The relative fluorescence (%) of AOB was influenced by the oxygen reduction metabolism. It peaked during Fe^{3+} reduction. In unreduced soil, the relative fluorescence of these TRFs varied from 9.33 to 19.33%. The relative fluorescence of *Nitrosospira* was low and *Nitrosomonas* was high. During Fe^{3+} reducing phase, the relative fluorescence of *Nitrosospira* was 14%, while that of *Nitrosomonas* and *Nitrososcoccus* was 48 and 31.33%, respectively. Relative fluorescence of AOA varied significantly during the course of soil reduction. The *Crenarchaeota* clade 1.1a and *Crenarchaeota* clade 1.1b had relative fluorescence of 9.33 to 12.67% before initiation of redox process. The relative fluorescence of these two TRFs increased to 33.33 and 53.67%, respectively, during incubation.

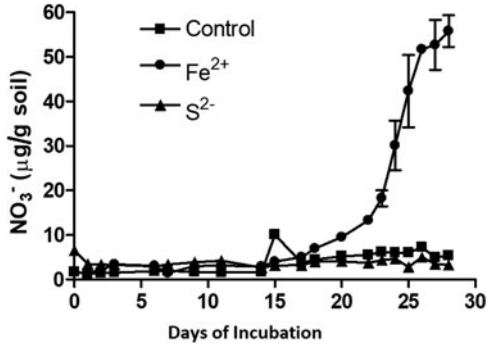

Fig. 4. Effect of electron donors on nitrification in a vertisol. Slurry samples were incubated with NH_4^+ as NH_4Cl (10 mM). The electron donor was either Fe^{2+} (sphere), or S^{2-} (triangle) at 10 mM concentration. Soil without any amendment served as control (square). *Y*-axis represents NO_3^- concentration, *X*-axis represents incubation period in days. Each datapoint represents arithmetic mean of three replicated observations with standard deviation as error bar.

Statistical interpretation

The effect of redox species (NO_3^-, Fe^{2+}, SO_4^{2-}, CH_4) on PNR and TRFs is shown in Table 3. Concentration of NO_3^- had a positive ($P < 0.05$) relationship with PNR, TRF 56 and TRF 247 ($P < 0.001$). Similarly, Fe^{2+} was positively ($P < 0.001$) related to PNR, TRF 219, TRF 56 and TRF 247. Change in SO_4^{2-} concentration was significantly ($P < 0.05$) related to TRF 56 and TRF 247. Headspace CH_4 was significantly ($P < 0.01$) related to TRF 48. The relationship between PNR and the variables was analysed by linear regression

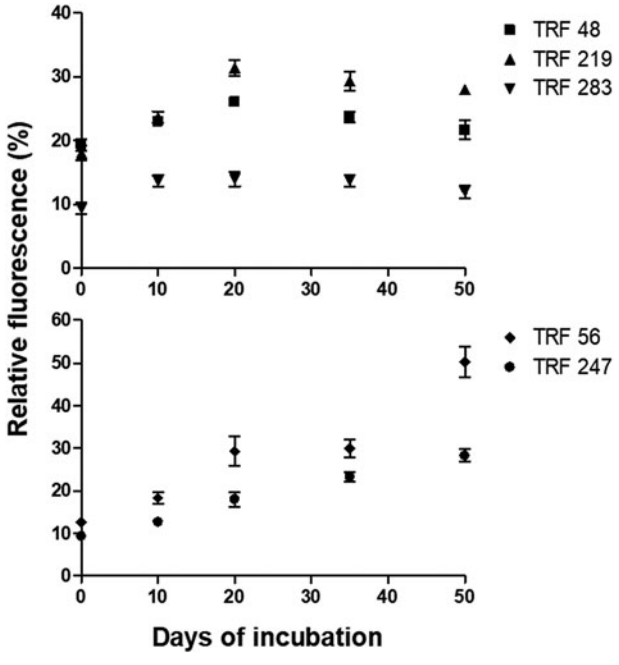

Fig. 5. Relative fluorescence of terminal restriction fragments (TRFs) indicative of AOA gene (alpha subunit of *amoA*) in slurry samples during redox metabolism. The TRFs of 48 bp, 219 bp, and 283 bp represented ammonia oxidizing bacteria (top). TRFs of 56 bp and 247 bp represented ammonia-oxidizing archaea (bottom). Each datapoint is arithmetic mean and standard deviation as error bar of three replicated observation. *Y*-axis represents relative fluorescence of TRFs, *X*-axis represents sampling period in days.

https://doi.org/10.1017/S0021859618000266 Published online by Cambridge University Press

Table 3. Effect of redox species (NO_3^-, Fe^{2+}, SO_4^{2-}, CH_4) on potential nitrification rate (PNR), relative fluorescence of ammonia-oxidizing bacteria (TRF 48, TRF 219, TRF 283) and ammonia-oxidizing archaea (TRF 56, and TRF 247)

	NO_3^-		Fe^{2+}		SO_4^{2-}		CH_4	
Parameters	*F*	*P*	*F*	*P*	*F*	*P*	*F*	*P*
PNR	5.398	0.034	44.34	<0.001	2.995	0.103	2.995	0.103
TRF 48	2.119	0.165	0.271	0.61	2.538	0.078	2.433	0.632
TRF 219	0.092	0.765	3.83	0.025	0.379	0.547	0.092	0.765
TRF 283	0.224	0.642	0.826	0.377	0.393	0.539	2.378	0.143
TRF 56	72.56	<0.001	85.54	<0.001	27.01	<0.001	3.082	0.011
TRF 247	40.09	<0.001	101.7	<0.001	14.74	0.001	3.54	0.011

Analysis of variance (ANOVA) with F and *P* values were estimated using the aov (parameter~factor) command in the console of R statistical program. High F and low *P* values indicate a significant level of impact. For all samples $n = 3$.
NO_3^-, nitrate; Fe^{2+}, ferrous iron; SO_4^{2-}, sulphate; CH_4, methane.

model (Fig. 6). The model indicated a significant linear relationship between PNR and NO_3^- ($P < 0.001$), Fe^{2+} ($P < 0.001$), TRF 219 ($P < 0.001$), TRF 56 ($P < 0.05$) and TRF 247 ($P < 0.05$). However, the regression model was not significant with SO_4^{2-}or CH_4. A multiple regression analysis predicted PNR as 0.303 NO_3^- (μM/g) + 0.661 Fe^{2+} (μM/g) − 0.629 SO_4^{2-} (μM/g) − 0.074 CH_4 (μg/g). The predicted nitrification correlated significantly with the observed values ($r^2 = 0.82$, $P < 0.001$).

The relative interaction among the variables was evaluated by a PCA biplot (Fig. 7). Principle component analysis of the data matrix resulted in most of the data variance being explained by the first two principal components. The first component explained 72.90% of the total variance, while 19.52% of the variance was explained by the second component. The PCA revealed thats Fe^{2+}, TRF 56 and TRF 247 were associated with PNR, while SO_4^{2-} and CH_4 exhibited the opposite interaction.

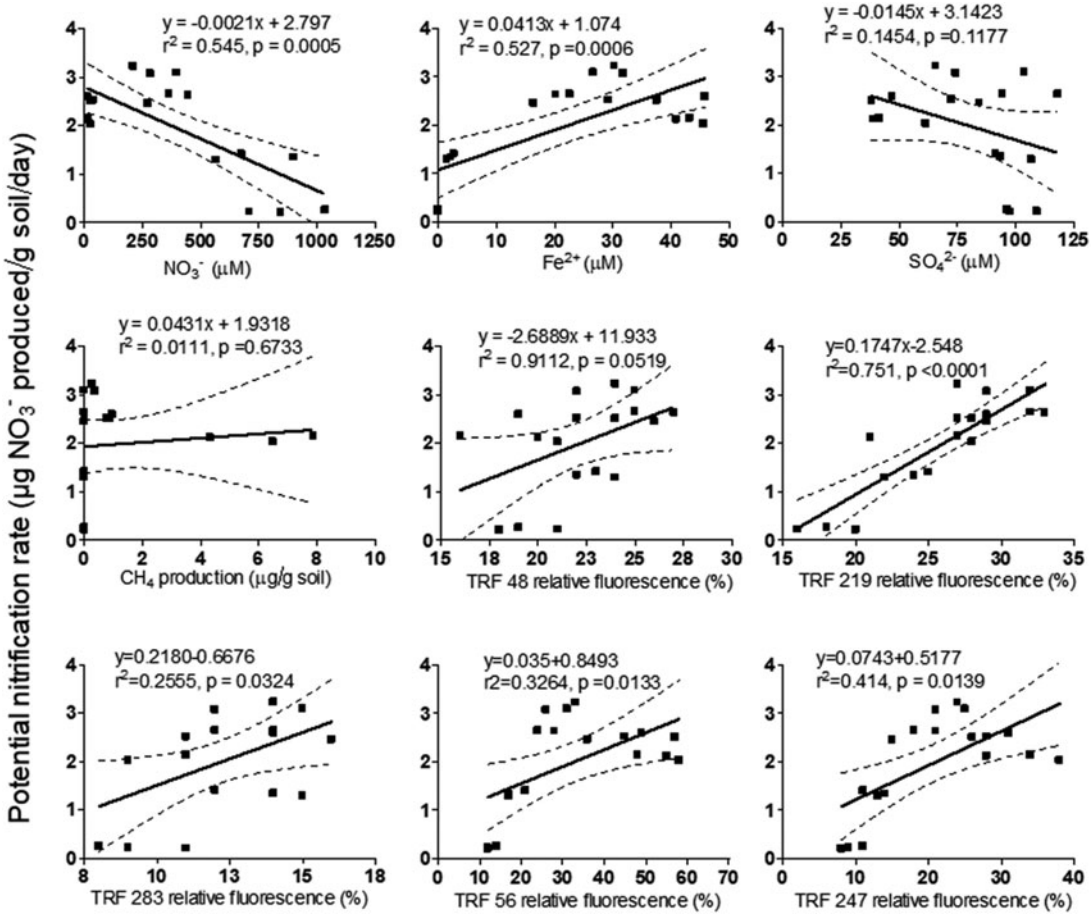

Fig. 6. Linear regression model (α 0.05) to predict potential nitrification rate from different parameters like concentration of terminal electron acceptors and microbial abundance. *Y*-axis represents potential nitrification rate and *X*-axis represents parameters corresponding to the plots.

https://doi.org/10.1017/S0021859618000266 Published online by Cambridge University Press

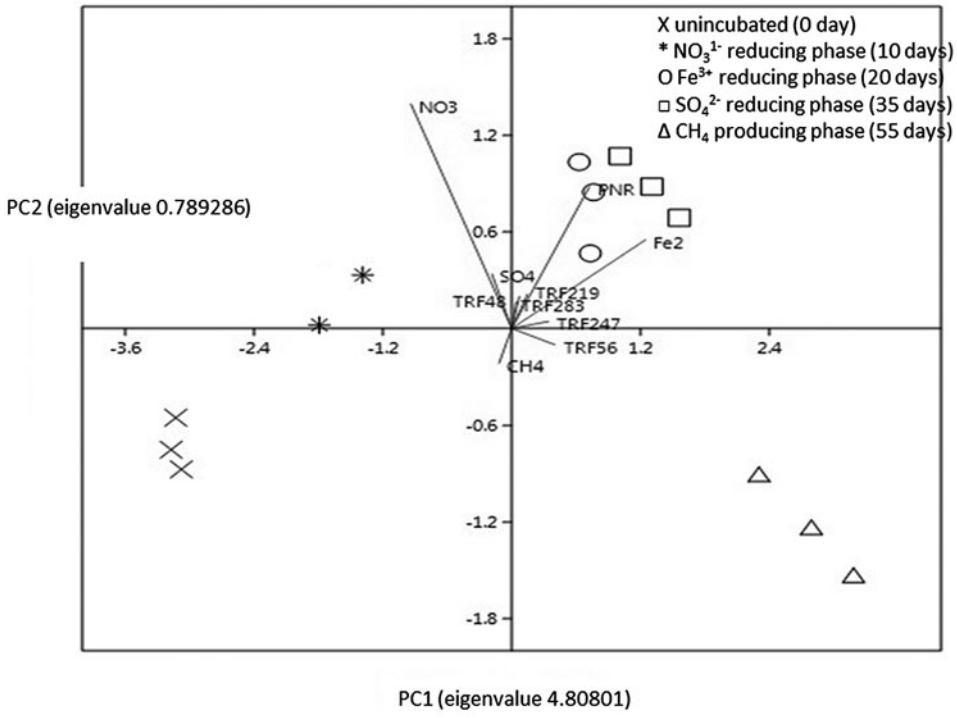

Fig. 7. PCA biplot with vectors of variables (lines) and factors. PC1 contributed 72.84% variation and PC2 contributed 19.45% variation. The factors are incubation period: 0 day (cross), 10 days (star), 20 days (circle), 35 days (square), and 55 days (triangle). The vectors (variables) are PNR, NO_3^-, Fe^{2+}, SO_4^{2-}, CH_4, TRF 48, TRF 219, TRF 283, TRF 56, and TRF 247. Vectors with narrow angles are strongly correlated; arrows that are perpendicular show no correlation while those of in opposite directions indicate negative correlation. More confidence characterizes comparisons between variables with longer lines, as inferences made from variables located near the centre of the diagram are often imprecise.

Discussion

Terminal electron-accepting process

The TEAPs followed the classical sequence of reduction of terminal electron acceptors. The sequential reduction of soil is generally carried out by different soil microbial groups (Patrick & Delaune 1972; Froelich *et al.* 1979). The consistency of sequential reduction indicated that soil samples were relatively homogeneous and inherent soil properties had a minimum contribution to the variations in reduction potentials (Gao *et al.* 2002; Tanji *et al.* 2003). Sequential reduction of the NO_3^-, Fe^{2+}, SO_4^{2-} and CO_2 overlapped during TEAPs. Microbial groups responsible for the reduction of different electron acceptors probably tend to overlap. Many anaerobes reduce more than one terminal electron acceptor. For example, many nitrate reducers are Fe^{3+} reducers and even some SO_4^{2-} reducers are methanogenic and also are capable of reducing Fe^{3+} (Coleman 1993; Lovley *et al.* 1993).

Nitrification during terminal electron-accepting process

Multiple regression model indicated that PNR was positively associated with nitrate and Fe^{2+} concentrations, negatively associated with SO_4^{2-} concentrations, and had no relationship with CH_4 concentrations. Slurry undergoing simultaneous denitrification and Fe^{3+} reduction exhibited high PNR because the regression coefficients of both electron acceptors were positive. Similarly, at the time of overlapping Fe^{3+} reduction and SO_4^{2-} reduction, nitrification proceeded because the coefficient of Fe^{2+} was higher than SO_4^{2-}. In general, slurry undergoing active denitrification and Fe^{3+} reduction resulted in high nitrification. On the contrary, nitrification was inhibited by SO_4^{2-} reduction and methanogenesis. It is likely that Fe^{2+} stimulated nitrification while S^{2-} inhibited it. Iron pyrite (FeS_2) has been found to inhibit nitrification in luvisols (Blaise *et al.* 1997). This is consistent with the observation in the current study that the reduced state of S produced during SO_4^{2-} reduction affected nitrification. Nitrification is a slow process compared to other aerobic microbial activities. Therefore, the nitrification progressed with a prolonged lag phase. The lag phase of autotrophic nitrifiers has been studied in water, aquatic plants, sediments and slimes. The lag phase of these samples varied from 20 to 55 days (Matulewich *et al.* 1975). Slow growth of nitrifiers and the rate-limiting factor for conventional biological removal of N compounds from water treatment plants has also been reported earlier (Zhou *et al.* 2014*a*).

Effect of electron donors on nitrification

Stimulation of nitrification by Fe^{2+} can be explained by three mechanisms: (1) Fe^{3+} acts as an electron acceptor and mediates NH_4^+ oxidation. Slurries were incubated aerobically but the occurrence of microaggregates cannot be ruled out. These microaggregates probably acted as sites for Fe^{3+} reducing NH_4^+ oxidation. (2) High CO_2 produced from the soil by amendment of Fe^{2+} stimulated nitrification. Carbon dioxide serves as the substrate for autotrophic nitrifiers and stimulates nitrification. The positive effect of CO_2 on autotrophic nitrifiers has been reported earlier (Kox & Jetten 2015). In soil, CO_2 is produced from organic matter decomposition. Soil micro-aggregates could be the source of CO_2 originating from the Fe^{3+} reduction coupled organic matter oxidation. (3) A third hypothesis is based on the fact that Fe^{2+}/Fe^{3+} cycling altered the soil physical properties. For example, conversion of Fe^{2+} to Fe^{3+} results in the formation of minerals of the high surface area (as Fe_2O_3). These minerals probably stimulated aerobic nitrification. In nature, iron oxides are ubiquitous reactive constituents of soils, sediments and aquifers. These minerals have extensive surface area and bind to an array of trace metals, nutrients and organic molecules (Li *et al.* 2014). The current results also revealed that nitrification was inhibited during SO_4^{2-} reduction or in the presence of the electron donor S^{2-}. This may have been due to competitive inhibition of nitrification by S^{2-}

https://doi.org/10.1017/S0021859618000266 Published online by Cambridge University Press

for O_2. The negative effect of S^{2-} on nitrifiers has been observed in wastewater treatment. In previous studies, it has been observed that S^{2-} at 0.5 mg/l inhibited nitrification by 30–40% (Kuenen & Robertson 1993; Zhou *et al.* 2014*b*).

Terminal-restriction fragment length polymorphism analysis

Microbial diversity in different terrestrial ecosystems has been explored by TRFLP. The TRFs retrieved covered various groups of AOB and AOA. These groups have been reported in plant rhizospheres (Park & Noguera 2004; Siripong & Rittmann 2007), meadow (Mintie *et al.* 2003), grassland (Horz *et al.* 2000) and agricultural soils. A TRF of 48 bp and 219 bp has been identified as representative of *Nitrososmonas* lineage, while a TRF 283 bp as *Nitrosospira* lineage (Park & Noguera 2004). Similarly, TRFs indicative of AOA have been found in temperate forest soil (Szukics *et al.* 2012). All three TRFs of AOB had similar relative fluorescence during the course of soil reduction. Relative fluorescence of AOB was high during NO_3^- and Fe^{3+} reduction and low during SO_4^{2-} reduction and CH_4 production. The reduced S molecules (S^{2-}) could have inhibited AOB (Elliott *et al.* 1998; Rittle *et al.* 1995). Under anaerobic conditions, metal sulphides (MS^-) are precipitated and immobilized (Moore *et al.* 1988; Zhang & Millero 1994). These MS^- inhibit many aerobic (Joye & Hollibaugh 1995) and anaerobic microorganisms (McCartney & Oleszkiewicz 1991). Relative fluorescence of AOA indicative TRFs increased consistently, due to the predominance of archaeal populations during redox metabolism. Therefore, the current study highlighted that AOA probably carried out nitrification during redox metabolism. Secondly, the adverse conditions for AOB due to the accumulation of S^{2-} resulting from SO_4^{2-} reduction probably favoured AOA. Nitrification is generally carried out by both AOB and AOA, although nitrifying bacteria are more dominant than the archaea. Thus, when the abundance of AOB was inhibited by reduced S molecules, the abundance of AOA increased to carry out nitrification.

The ANOVA showed that NO_3^- and Fe^{2+}AOA influenced PNR and archaeal TRFs positively, while SO_4^{2-} and CH_4 has a positive influence on the archaeal TRFs. Thus, AOB probably regulated nitrification during the initial reductive phases, while AOA carried out nitrification at the later stage of soil reduction (SO_4^{2-} reduction and methanogenic). Regression models of PNR varied positively with Fe^{2+} and crenarchaeal population. Derivation of regression models with different soil types would provide a better prediction model for the PNR. Polymerase chain reaction defined the type and magnitude of relation among the variables. The results of the current study confirmed that nitrification in flooded soil ecosystems is a complex phenomenon, which is carried out by both nitrifying bacteria and archaea. Based on the results a hypothetical pathway is illustrated to depict the nitrification carried out by the nitrifying bacteria and nitrifying archaea in flooded soil ecosystem (Fig. 8). Dissolved oxygen concentration in the slurries as well as in the headspace of the microcosms varies with redox metabolism. For example, the oxygen level or the extent of anaerobiosis (redox potential or Eh) is higher in the later phase than the early phases of reduction. This could be the major factor that influenced nitrification. It is concluded that bacteria modulate nitrification during the early phase of soil reduction while archaea steer nitrification at the later stages of redox metabolism in vertisols.

Conclusion

Nitrification in flooded soil is a complex process governed by different microbial groups and terminal electron acceptors. The current experiment highlighted that nitrification is stimulated during reduction of $NO_3^-$and Fe^{3+} and inhibited during SO_4^{2-} reduction and methanogenic phases. Multiple regression analysis predicted nitrification from the rates of redox metabolic processes. Thus, at the time of overlapping of NO_3^-/Fe^{3+} reduction and Fe^{3+}/ SO_4^{2-} reduction, nitrification proceeded in a forward direction. The Fe^{3+} reducing slurries enhanced nitrification. According to the results of the present study, it is predicted that slurries at the Fe^{3+} reducing phase have Fe^{3+} reduction dependent nitrification and probably both aerobic and anaerobic nitrification stimulate the net nitrification activity. This needs to be investigated further. The current study also revealed that nitrification in the flooded soil is likely to be driven by both AOB and AOA. Both actively nitrify during NO_3^- reduction and Fe^{3+} reduction. Archaea regulated nitrification at SO_4^{2-} reduction and the methanogenic phase. However, the complex microbial interaction needs to be verified in other soil types. It is predicted that climate change is likely to increase atmospheric temperatures in the near future. This may lead to intensive precipitation in many areas in the tropics. Large upland areas will remain submerged depending on the precipitation intensity, which would create anoxic-oxic fluctuations in soils. Based on the current study, anoxic–oxic conditions are likely to enhance nitrification in tropical vertisols. High nitrification may aggravate N loss through N_2O emission or leaching. This may complicate the problems affecting

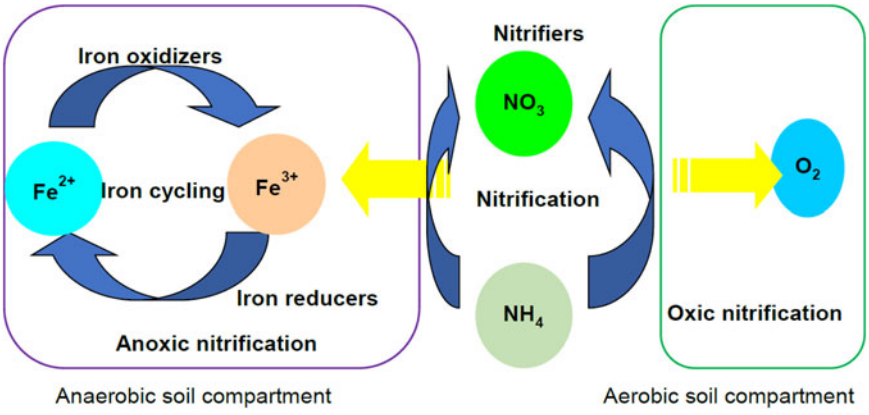

Fig. 8. Nitrification pathways in the flooded soil ecosystem. Nitrification occurs aerobically in presence of O_2 as the electron (e^-) acceptor. Aerobic nitrification takes place in the oxic compartments of soil. In anaerobic soil, the anoxic compartments including microaggregates serve as sites for anaerobic NH_4 oxidation. It is hypothesized that slurries undergoing Fe^{3+} reducing phase likely stimulate nitrification by coupling NH_4 oxidation with Fe^{3+} reduction.

https://doi.org/10.1017/S0021859618000266 Published online by Cambridge University Press

agriculture, climate and environment. Further studies are essential to exhibit the complex interaction between oxygen reduction metabolism and nitrification in agricultural field to better predict the N dynamics and influence on the ecosystem.

Acknowledgements. This manuscript is part of the project 'Archaea and Actinobacteria in Vertisol of Central India – Diversity, Biogeochemical Processes and Bioinoculants' funded by ICAR-AMAAS.

Conflict of interest. None.

References

Blaise D, Amberger A and von Tucher S (1997) Influence of iron pyrites and dicyandiamide on nitrification and ammonia volatilization from urea applied to loess brown earths (luvisols). *Biology and Fertility of Soils* **24**, 179–182.

Caffrey JM (1995) Spatial and seasonal patterns in sediment nitrogen remineralization and ammonium concentrations in San Francisco Bay, California. *Estuaries* **18**, 219–233.

Coleman ML (1993) Microbial processes: controls on the shape and composition of carbonate concretions. *Marine Geology* **113**, 127–140.

Davidson EA and Janssens IA (2006) Temperature sensitivity of soil carbon decomposition and feedbacks to climate change. *Nature* **440**, 165–173.

de Mendiburu F (2014) *Agricolae: Statistical Procedures for Agricultural Research*. R Package Version 1.1-6. Lima Peru: The Comprehensive R Archive Network.

Elliott P, Ragusa S and Catcheside D (1998) Growth of sulphate-reducing bacteria under acidic conditions in an upflow anaerobic bioreactor as a treatment system for acid mine drainage. *Water Research* **32**, 3724–3730.

Flood M, *et al.* (2015) Ammonia-oxidizing bacteria and archaea in sediments of the Gulf of Mexico. *Environmental Technology* **36**, 124–135.

Francis CA, *et al.* (2005) Ubiquity and diversity of ammonia-oxidizing archaea in water columns and sediments of the ocean. *Proceedings of the National Academy of Sciences USA* **102**, 14683–14688.

Froelich PN, *et al.* (1979) Early oxidation of organic matter in pelagic sediments of the eastern equatorial Atlantic: suboxic diagenesis. *Geochimica et Cosmochimica Acta* **43**, 1075–1090.

Gao S, *et al.* (2002) Comparison of redox indicators in a paddy soil during rice-growing season. *Soil Science Society of America Journal* **66**, 805–817.

Gribaldo S, *et al.* (2010) The origin of eukaryotes and their relationship with the Archaea: are we at a phylogenomic impasse? *Nature Reviews Microbiology* **8**, 743–752.

Horz H-P, *et al.* (2000) Identification of major subgroups of ammonia-oxidizing bacteria in environmental samples by T-RFLP analysis of *amoA* PCR products. *Journal of Microbiological Methods* **39**, 197–204.

Ihaka R and Gentleman R (1996) R: a language for data analysis and graphics. *Journal of Computational and Graphical Statistics* **5**, 299–314.

Isobe K, *et al.* (2012) High abundance of ammonia-oxidizing archaea in acidified subtropical forest soils in southern China after long-term N deposition. *FEMS Microbiology Ecology* **80**, 193–203.

Jackson ML (1958) *Soil Chemical Analysis*. Englewood, Cliffs, NJ: Prentice-Hall, Inc.

Joye SB and Hollibaugh JT (1995) Influence of sulphide inhibition of nitrification on nitrogen regeneration in sediments. *Science* **270**, 623–625.

Jung M-Y, *et al.* (2011) Enrichment and characterization of an autotrophic ammonia-oxidizing archaeon of mesophilic crenarchaeal group I. 1a from an agricultural soil. *Applied and Environmental Microbiology* **77**, 8635–8647.

Kowalchuk GA, *et al.* (2000) Changes in the community structure of ammonia-oxidizing bacteria during secondary succession of calcareous grasslands. *Environmental Microbiology* **2**, 99–110.

Kox MA and Jetten MSM (2015) The nitrogen cycle. In Lugtenberg B (ed.). *Principles of Plant-Microbe Interactions*. Berlin, Germany: Springer, pp. 205–214.

Kuenen JG and Robertson LA (1993) The use of natural bacterial populations for the treatment of sulphur-containing wastewater. In Rosenberg E (ed.). *Microorganisms to Combat Pollution*. Dordrecht, The Netherlands: Springer, pp. 115–130.

Leininger S, *et al.* (2006) Archaea predominate among ammonia-oxidizing prokaryotes in soils. *Nature* **442**, 806–809.

Li JJ, *et al.* (2014) Effects of groundwater geochemical constituents on degradation of benzene, toluene, ethylbenzene, and xylene coupled to microbial dissimilatory Fe (III) reduction. *Environmental Engineering Science* **31**, 202–208.

Lovley DR, *et al.* (1993) *Geobacter metallireducens* gen. nov. sp. nov., a microorganism capable of coupling the complete oxidation of organic compounds to the reduction of iron and other metals. *Archives of Microbiology* **159**, 336–344.

Matulewich VA, Strom PF and Finstein MS (1975) Length of incubation for enumerating nitrifying bacteria present in various environments. *Applied Microbiology* **29**, 265–268.

McCartney DM and Oleszkiewicz JA (1991) Sulphide inhibition of anaerobic degradation of lactate and acetate. *Water Research* **25**, 203–209.

Mintie AT, *et al.* (2003) Ammonia-oxidizing bacteria along meadow-to-forest transects in the Oregon Cascade Mountains. *Applied and Environmental Microbiology* **69**, 3129–3136.

Mohanty SR, *et al.* (2014) Methane oxidation and methane driven redox process during sequential reduction of a flooded soil ecosystem. *Annals of Microbiology* **64**, 65–74.

Moore JN, Ficklin WH and Johns C (1988) Partitioning of arsenic and metals in reducing sulfidic sediments. *Environmental Science and Technology* **22**, 432–437.

Oksanen J, *et al.* (2007) *The vegan Package. Community Ecology Package*, version 1.8-8. Finland: The Comprehensive R Archive Network.

Park H-D and Noguera DR (2004) Evaluating the effect of dissolved oxygen on ammonia-oxidizing bacterial communities in activated sludge. *Water Research* **38**, 3275–3286.

Patrick WH and Delaune RD (1972) Characterization of the oxidized and reduced zones in flooded soil. *Soil Science Society of America Journal* **36**, 573–576.

Radax R, *et al.* (2012) Ammonia-oxidizing archaea as main drivers of nitrification in cold-water sponges. *Environmental Microbiology* **14**, 909–923.

Rittle KA, Drever JI and Colberg PJS (1995) Precipitation of arsenic during bacterial sulphate reduction. *Geomicrobiology Journal* **13**, 1–11.

Schmidt EL and Belser LW (1982) Nitrifying bacteria. In Page AL, Miller RH and Keeney DR (eds). *Methods of Soil Analysis, Part2: Microbiological and Biochemical Properties* Madison, WI: ASA, SSSA, pp. 1027–1042.

Searle PL (1979) Measurement of adsorbed sulphate in soils – effects of varying soil: extractant ratios and methods of measurement. *New Zealand Journal of Agricultural Research* **22**, 287–290.

Shyu C, *et al.* (2007) MiCA: a web-based tool for the analysis of microbial communities based on terminal-restriction fragment length polymorphisms of 16S and 18S rRNA genes. *Microbial Ecology* **53**, 562–570.

Siripong S and Rittmann BE (2007) Diversity study of nitrifying bacteria in full-scale municipal wastewater treatment plants. *Water Research* **41**, 1110–1120.

Stookey LL (1970) Ferrozine – a new spectrophotometric reagent for iron. *Analytical Chemistry* **42**, 779–781.

Szukics U, *et al.* (2012) Rapid and dissimilar response of ammonia oxidizing archaea and bacteria to nitrogen and water amendment in two temperate forest soils. *Microbiological Research* **167**, 103–109.

Tanji KK, *et al.* (2003) Characterizing redox status of paddy soils with incorporated rice straw. *Geoderma* **114**, 333–353.

Tourna M, *et al.* (2011) *Nitrososphaera viennensis*, an ammonia oxidizing archaeon from soil. *Proceedings of the National Academy of Sciences of the United States of America* **108**, 8420–8425.

Treusch AH, *et al.* (2005) Novel genes for nitrite reductase and Amo-related proteins indicate a role of uncultivated mesophilic crenarchaeota in nitrogen cycling. *Environmental Microbiology* **7**, 1985–1995.

Walther GR, *et al.* (2002) Ecological responses to recent climate change. *Nature* **416**, 389–395.

Watson SW, *et al.* (1986) *Nitrospira marina* gen. nov. sp. nov.: a chemolithotrophic nitrite-oxidizing bacterium. *Archives of Microbiology* **144**, 1–7.

Yang Y, *et al.* (2016) Ammonia-oxidizing archaea and bacteria in water columns and sediments of a highly eutrophic plateau freshwater lake. *Environmental Science and Pollution Research International* **23**, 15358–15369.

Ying J-Y, Zhang L-M and He J-Z (2010) Putative ammonia-oxidizing bacteria and archaea in an acidic red soil with different land utilization patterns. *Environmental Microbiology Reports* **2**, 304–312.

Zhang JZ and Millero FJ (1994) Investigation of metal sulfide complexes in sea water using cathodic stripping square wave voltammetry. *Analytica Chimica Acta* **284**, 497–504.

Zhou M, Ye H and Zhao X (2014*a*) Isolation and characterization of a novel heterotrophic nitrifying and aerobic denitrifying bacterium *Pseudomonas stutzeri* KTB for bioremediation of wastewater. *Biotechnology and Bioprocess Engineering* **19**, 231–238.

Zhou Z, *et al.* (2014*b*) Inhibitory effects of sulfide on nitrifying biomass in the anaerobic–anoxic–aerobic wastewater treatment process. *Journal of Chemical Technology and Biotechnology* **89**, 214–219.

https://doi.org/10.1017/S0021859618000266 Published online by Cambridge University Press